JOURNAL OF CATALYSIS 146, 40–55 (1994)

Isobutane Dehydrogenation over Sulfided Nickel Catalysts

Daniel E. Resasco,[1] Bonnie K. Marcus, Chen S. Huang, and Vincent A. Durante[2]

Research and Development Department, Sun Company, Inc., P.O. Box 1135, Marcus Hook, Pennsylvania 19061-0835

Received June 22, 1993 revised September 22, 1993

We have studied the dehydrogenation of isobutane to isobutylene over heavily sulfided Ni catalysts at 873 K. In the absence of sulfur but in the presence of hydrogen, supported metallic nickel catalyzes the rapid hydrogenolysis of alkanes, resulting in exceedingly poor selectivity toward dehydrogenation products. However, the hydrogenolysis activity can be essentially eliminated by proper sulfidation, resulting in high selectivity toward isobutylene production. Due to thermodynamic limitations, elevated temperatures are necessary to attain reasonable conversions to isobutylene. Under these conditions, the formation of coke is rapid and is the main cause of catalyst deactivation. Treatment of nickel catalysts with relatively large amounts of sulfur-containing reagents results not only in dramatically improved selectivity but also in a decreased rate of coke formation. The catalysts exhibited activation periods of several hours until a maximum was reached when they were placed in the reaction environment at 873 K. This activation period did not depend upon the previous reduction treatment but did depend upon the time on stream. A correlation was found between the increase in activity and the growth of a carbidic phase on the catalyst. This species, characterized by TPO and XPS, reached a saturation value at a C/Ni ratio of unity, which was coincidental with the amount of carbon on the catalyst when it achieved its maximum activity. Two alternative explanations for the activation process are discussed. The first considers the participation of a nickel–carbidic–carbon complex in the reaction scheme. The second considers the creation of sulfur vacancies during the initial coke deposition period which would increase the exposure of a catalytically active Ni–S moiety.

INTRODUCTION

The increasing demand for certain olefins as chemical intermediates for the production of oxygenates and alkylates for motor fuels, coupled with the plentiful supply of lower alkanes, provides incentive for the use of catalytic dehydrogenation on an industrial scale (1). Driven largely by the rapid growth in demand for tertiary alkyl ethers, the dehydrogenation of isobutane or isopentane to isobutylene or isoamylene, respectively, is receiving renewed attention since branched ethers are prepared by etherification of branched olefins with methanol or ethanol.

The dehydrogenation reaction is currently carried out in commercial processes in the vapor phase over chromia–alumina or noble-metal catalysts. Due to the endothermic nature of this reaction and the normally unfavorable equilibrium, elevated process temperatures are necessary to reach economically acceptable levels of conversion. These severe operating conditions favor coke formation and catalyst deactivation. As a consequence, most of the commercial processes for dehydrogenation of lower alkanes require feeds diluted with hydrogen or steam and short reaction cycles with frequent regenerations (1, 2). Improved process economics could result from the development of catalysts that perform well under severely deactivating conditions.

Previous workers have shown that the addition of small amounts of S has beneficial effects on selectivity and coke formation. For example, Rennard and Freel (3) have shown that sulfur causes an increase in propylene yield over Pt–Re catalysts increased upon sulfiding. The effect of sulfur in reducing the rate of coke formation has been reported by Rostrup-Nielsen and co-workers (5–7, 14, over Pt–Re catalysts increased upon sulfiding. The effect of sulfur in reducing the rate of coke formation has been reported by Rostrup-Nielsen and co-workers (5–7, 14, 15) for the case of steam reforming of CH_4. The presence of half a monolayer of sulfur on the Ni surface strongly inhibited the rate of carbon deposition, while it did not inhibit the rate of steam reforming to the same extent. This effect has been explained in terms of the ensemble of atoms required to constitute the active site for each reaction. The ensemble for the steam reforming reaction is smaller than that required for coke formation. Consequently, although both rates decreased when sulfur was added, the coking rate did so almost 10 times faster than the reforming rate.

In this paper, we describe the use of heavily sulfided nickel catalysts supported on nonacidic aluminas for the dehydrogenation of isobutane. We have demonstrated that versions of these catalysts are active and selective

[1] Current address: School of Chemical Engineering and Material Science, University of Oklahoma, 100 E. Boyd St., Norman, OK 73019-0628.

[2] To whom correspondence should be addressed.

0021-9517/94 $6.00

TABLE 1

Characteristics of the Catalysts Investigated

Catalyst	Calcination of support	Metal (wt%)	Alkali (wt%)	Thermal Treatment	Dispersion (H/M)
A	1223 K (10 hr)	6% Ni	5% Cs	Red. 873 K	0.35
B	1223 K (10 hr) leached w/acid	6% Ni	5% Cs	Red. 873 K	0.34
C	1223 K (10 hr)	6% Ni	3% Cs	Red. 873 K	ND
D	NONE	6% Ni	5% Cs	Red. 873 K	ND
E	1223 K (10 hr)	3% Ni	5% Cs	Red. 873 K	0.5
F	1223 K (10 hr)	6% Ni	5% Cs	Oxid. 623 K	ND
G	1223 K (10 hr)	0.35% Pt 1% Sn	8% K	Red. 873 K	0.85

for relatively long reaction times under low hydrogen/hydrocarbon ratios, resulting in an important advantage compared to the existing technology. We view the heavily sulfided nickel component present in these catalysts as a compound with different properties from those of metallic nickel rather than as a zero-valent metal modified by the presence of chemisorbed sulfur.

II. EXPERIMENTAL

Catalytic Materials

Table 1 summarizes the differences in the various preparations reported in this work, i.e., the amount of Ni, the amount of Cs, the calcination of the support, and the thermal pretreatment of the catalysts. The material used as a support for the catalysts reported here was γ-alumina (CS331-4 from United Catalysts), ground and sieved to 18/35 mesh. Before any further treatment, the alumina was calcined in air at 1223 K for 10 hr. X-Ray diffraction powder patterns of the calcined material revealed a transformation to the theta phase. During this transformation, the BET surface area, as determined by nitrogen adsorption conducted in a Coulter Omnisorp 360 instrument, changed from 225 m^2/g for the fresh material to 130 m^2/g for the calcined support.

In one of the samples, catalyst D, the precalcination treatment was omitted. In another sample, catalyst B, the alumina support was treated with a 1.0 *M* aqueous oxalic acid solution for 2 h at 348 K in order to increase the pore volume in the 10 to 20 nm pore radius range, as described later. To reduce the acidity, each alumina support was impregnated with an aqueous solution of $CsNO_3$ using a liquid/solid ratio of 0.65 ml/g, and then dried in an oven at 423 K. The resulting cesium content was 5 wt% in all the samples except for catalyst C, in which it was 3 wt%. Loading with Ni was accomplished by incipient wetness impregnation using a solution of $Ni(NO_3)_2 \cdot 6\ H_2O$ in acetone, keeping the liquid/solid ratio at 0.65 ml/g. The volume of liquid used corresponds to the total pore volume of the calcined support, as measured by nitrogen desorption porosimetry. The resulting material was dried in an oven at 423 K. The nominal Ni loading was 6 wt% in all the samples except in catalyst E in which it was 3 wt%. The sulfiding of the samples was done *in situ* as described below.

Before each run, the catalyst was placed in a packed bed reactor and reduced in pure hydrogen with a temperature ramp of 3 K/min up to 543 K and held at that temperature for two hours then further heated at 3K/min up to 873 K. One hour later, the catalyst was presulfided by injecting measured quantities of dimethyl sulfoxide (DMSO) into the preheater section into a hydrogen stream. Unless otherwise specified, the amount of DMSO injected in each case corresponded to a S/bulk Ni molar ratio of 1/2. Additional sulfiding agents were studied in separate experiments.

In one of the samples, catalyst F, the reduction treatment was omitted and the catalyst was preoxidized at 523 K before sulfiding. In this case, the sulfiding was done *ex situ* in a quartz reactor in two steps. In the first step, the DMSO was added to the oxidized sample at 473 K at a S/bulk Ni molar ratio of 1/2. Then the temperature was raised to 673 K, followed by a similar injection of DMSO. Finally, the catalyst was flashed with hydrogen for 30 min, purged with nitrogen, passivated in a 1% O_2 atmosphere, and exposed to air.

For comparison with the sulfided nickel catalysts, an unsulfided bimetallic Pt–Sn catalyst (catalyst G) was prepared. This catalyst was prepared by impregnation on the same calcined alumina used for the nickel catalysts. The addition of Pt was accomplished by incipient wetness impregnation using an aqueous solution of hexachloroplatinic acid in a 0.65 ml/g liquid to solid ratio, the concentration of the solution being adjusted to yield a Pt loading of 0.35 wt%. The addition of Sn was accomplished by

impregnation with a solution of stannous chloride. The acidity of the support was then reduced by addition of potassium salts followed by heat treatments.

Catalyst Characterization

The catalysts and their precursors were characterized by several techniques. The metal dispersions were measured prior to sulfiding by temperature programmed desorption of adsorbed hydrogen in a AMI-1 Altamira instrument after reduction at 873 K for 2 hr and saturation with pure hydrogen at 303 K. The data obtained by TPD of adsorbed hydrogen were calibrated against the volumetric hydrogen uptake measured for one of the samples using an Omnisorp 360 operating in static chemisorption mode. Once sulfided, an XPS technique described later was used to guage relative dispersion of nickel sulfide species. To obtain a relative measure of the acidity of the support we used TPD of pyridine adsorbed at room temperature to saturation.

The pore size distributions of fresh and spent catalysts were determined by a standard nitrogen desorption technique in an Omnisorp 360 using a cylindrical pore model. The carbon deposits were analyzed by temperature programmed oxidation (TPO) and reduction (TPR) in a quartz reactor directly connected to a thermal conductivity detector and a Hewlett Packard quadrupole mass spectrometer. The combustion of the carbon deposits was also studied in a Dupont 990 Differential Scanning Calorimeter. The coke morphology was investigated by transmission electron microscopy (TEM) in a Phillips TEM at the University of Delaware. The electron microscope specimens were prepared from heavily coked samples slurried in ultrasonically stirred propanol and deposited on gold grids. After evaporating the propanol, the powder was well dispersed over the grid.

The nature of the carbon deposits was further investigated by X-ray photoelectron spectroscopy. The XPS studies were conducted using a Kratos Xsami instrument equipped with a dual-anode X-ray source and a reactor for *in situ* treatments. Binding energy measurements were referenced to Al(2*s*) = 119.2 eV. Data reduction was carried out using the Vision software provided by Kratos. XPS was also used to study the effects on the nature and dispersion of the Ni–S species of reduction and oxidation pretreatments before sulfiding. X-ray diffraction powder patterns of the catalysts were obtained on a Scintag Pad IV X-ray diffractometer. A commercial software package was used to control aquisition and reduction of the data.

Activity Measurements

Catalytic activity data were obtained in two different reactors. A downflow tubular reactor was used for catalyst life on-stream studies and a recirculating reactor was used for kinetics studies. The tubular reactor had passivated stainless steel walls with an internal diameter of $\frac{1}{2}$ in. Passivation was accomplished by repeated exposure of the empty reactor to H_2S, DMSO, and H_2 mixtures at 873 K prior to activity measurements. The catalyst bed volume was constant for all the runs at 17 cm^3. For runs used to study nonsulfided catalysts, nonpassivated reactors constructed of 316 stainless steel were used. This reactor was operated isothermally at 873 K and controlled within 1 K by a temperature controller through a PID loop. Isobutane was fed through a liquid metering pump into a thermostated, packed preheating chamber. The isobutane gas flow was kept constant at 280 ml/min NTP. Hydrogen flow was controlled by a mass flow controller and varied from 0 to 560 ml/min NTP. As mentioned above, before each run the catalysts were reduced and sulfided with DMSO. After sulfiding, the catalyst was left under hydrogen at 873 K for an additional 1 hr before the introduction of the hydrocarbon feed. The hydrogen to hydrocarbon ratio was varied between 0 and 6. After each reaction run in the flow reactor, the total amount of carbon deposited on the catalyst was determined using a LECO carbon analyzer.

A stainless steel Berty type recirculating reactor from Autoclave Engrg. was used to determine kinetics parameters. The catalyst was held in a basket placed over a stirrer which could be operated at different speeds to vary the recirculation flow. Flow rates of isobutane, hydrogen, and argon were controlled by mass flow controllers. The reactor was operated in a differential mode. The total feed flow rate was kept constant at 100 ml/min NTP, while the recirculation flow rate was 15,000 ml/min NTP. Under these conditions, in which the recirculation flow rate was much higher than the feed flow rate, the concentration of reactants and products was essentially constant and the reactor could be considered a continuous stirred tank (8). In order to obtain reaction orders with respect to isobutane and hydrogen, the individual flow rates were varied while the total flow rate was kept constant. To determine activation energies, the temperature was varied from 823 to 703 K. As in the case of the flow reactor, before each run, the catalysts were reduced at 873 K for 1 hr and then sulfided by injecting DMSO into the hydrogen stream.

Rates of carbon formation were also obtained in this reactor. In those experiments, gaseous streams of isobutane, isobutylene, and hydrogen, controlled by mass flow controllers, were continuously co-fed into the stirred tank reactor at 873 K and a total flow rate of 100 ml/min NTP. After a given time in contact with a particular gaseous mixture, the reactor was cooled in Ar, and the amount of carbon on the catalyst was measured by the LECO method.

Reaction products from both reactors were analyzed

off line in a gas chromatograph. Selected gas samples were analyzed by GC-MS. The data from both analytical methods were in excellent agreement, and the reproducibility of the data obtained from different runs on the same sample was within 10%. The steady state conditions of the feed were reached in less than 15 min, but as described below, the catalysts exhibited activation periods of several hours before achieving their maximum activity.

III. RESULTS

Effect of Adding S to Ni Catalysts

In one of the Ni/Cs–Al_2O_3 samples, catalyst A, we varied the amount of sulfur injected before the reaction run and studied the consequential catalytic performance in the flow reactor. We observed, at 873 K, that the reduced but unsulfided Ni catalyst exposed to a 0.5 H_2/isobutane feed produced only methane and coked rapidly. On the other hand, as increasing amounts of DMSO were added to the prereduced Ni catalyst, both the hydrogenolysis and coking rates drastically decreased. As shown in Fig. 1, the carbon content measured after 10 hr on stream at 873 at a H_2/isobutane ratio of 0.5 dropped from almost 9 g C/g cat for the unsulfided Ni catalyst to almost 0 for catalyst exposed to a S/Ni ratio greater than 0.25. Likewise, the carbon molar selectivity towards methane decreased from 100% to less than 4%.

Although some weakly bound S-containing species may have desorbed after catalysts had been sulfided with DMSO then exposed to hydrogen, most of the S clearly remained on the catalyst. Analysis of one sample which had been subjected to a single sulfiding with DMSO at the start of the run indicated a residual sulfur to nickel ratio of 0.2 after 336 hr on stream. During the course of a separate experiment (using a catalyst with a lower nickel loading) in which H_2S had been used as a sulfiding agent and the hydrogen to hydrocarbon ratio increased to 6, S content noticeably dropped after only 10 h on stream. In this case, the time dependent product distribution was characterized by a loss of selectivity (increase in methane) with time. Such rapid selectivity loss was never observed when DMSO was used as a sulfiding agent and the hydrogen to hydrocarbon ratio was kept at 2 or less.

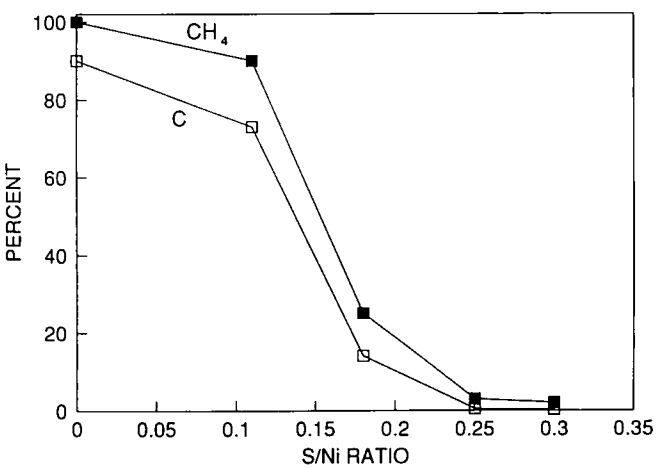

FIG. 1. Effect of sulfur on isobutane hydrogenolysis and coke formation over catalyst A (6% Ni/5% Cs–Al_2O_3). (■) Selectivity to methane as measured in the flow reactor at 873 K and a H_2/isobutane molar ratio of 1/2. (□) Carbon content on the catalyst after 10 hr under steady state reaction conditions.

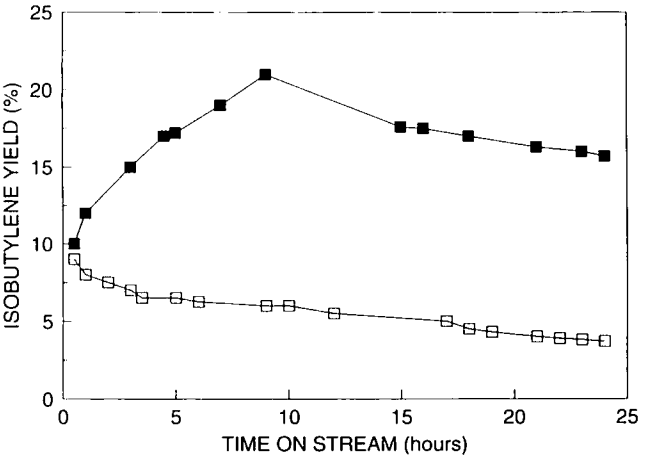

FIG. 2. Evolution of activity as a function of time on stream. H_2–isobutane reaction (molar ratio 1/2) at 873 K in the flow reactor. (■) Catalyst A (6% Ni/5% Cs–Al_2O_3). (□) Catalyst G (0.35% Pt-1% Sn/K–Al_2O_3).

Activity Variation as a Function of Time on Stream

The evolution of activity of the sulfided Ni catalysts was studied in the fixed-bed flow reactor under various conditions. For example, a series of reactions were carried out at 873 K using a gas hourly space velocity of 1330 hr^{-1}. Before starting each reaction, the catalysts were prereduced and sulfided at 873 K. The sulfiding agent, DMSO, was injected into the H_2 stream at a S/Ni molar ratio of 1/2.

Figure 2 illustrates the variation of the dehydrogenation reaction rate over catalyst A studied during a 24 hr reaction period. Over the course of the initial hours on stream, the conversion increased with time while the carbon selectivity toward isobutylene remained essentially constant at above 90%. It must be noted that this induction period, during which the catalyst activity increased, was observed for all the sulfided nickel catalysts investigated. It only occurred during the initial reaction run and after regeneration in air followed by rereduction and sulfiding. It did not occur when the reaction was stopped, left overnight in hydrogen at the same temperature, and then restarted. Data obtained over the unsulfided Pt/Sn/K-Al_2O_3 catalyst

TABLE 2

Kinetics Parameters Obtained on Catalyst E (3%Ni/5%Cs–Al2O3)

Reaction orders		Activation energy (kcal/mol)
Hydrogen	Isobutane	
0	0.9 ± 0.2	30 ± 3

TABLE 3

Correlation between Activity and XPS Intensity Ratios on Sulfided Nickel Catalysts

Catalyst	Reaction rate (mol/kg cat hr)	Ni/Al XPS ratio	S^{2-}/Al XPS ratio
A (red. 873 K + sulfided)	5.5	0.60	0.04
F (oxid. 623 K + sulfided)	9.3	0.86	0.08

are also included in Fig. 2. Contrasting with the activity evolution patterns displayed by the sulfided nickel catalysts, no activation period and a continuous deactivation were observed with the Pt catalyst.

Effect of Varying the Hydrogen/Hydrocarbon Feed Ratio

The kinetics parameters obtained on catalyst E for the dehydrogenation of isobutane are summarized in Table 2. The reaction order with respect to isobutane was found to be about 1 while the order with respect to hydrogen was 0. The activation energy was 30 ± 3 kcal/mole. We have studied the effect of the H_2/hydrocarbon ratio on both initial activity and deactivation rate. As shown in Fig. 3, due to the first order dependence of the reaction with the concentration of isobutane, the dehydrogenation rate decreased with an increase in the H_2/hydrocarbon ratio since the concentration of isobutane became diluted with hydrogen. On the other hand, the deactivation rate, as measured from the slope of conversion as a function of time on stream after the induction period and at comparable conversion levels, was not very sensitive to the hydrogen concentration. It only increased when the H_2/hydrocarbon ratios were close to 0.

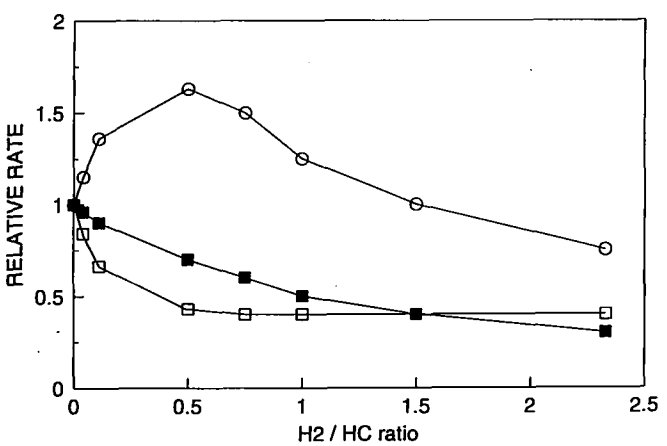

FIG. 3. Isobutane dehydrogenation and deactivation relative rates as a function of H_2–isobutane molar ratio. (■) Relative maximum rates of isobutane dehydrogenation. (□) Relative deactivation rate, measured after the activation period. (○) Performance ratio = dehydrogenation/deactivation.

By taking the ratio between the initial dehydrogenation and deactivation rates, a performance parameter can be obtained. The H_2/hydrocarbon ratio at which this parameter is maximum would represent the optimum run conditions. As illustrated in Fig. 3, the optimal operating conditions in the case of sulfided nickel catalysts would be at a H_2/isobutane ratio of about 0.5.

This behavior contrasts with that of a typical supported metallic Pt catalyst, for which the deactivation rate is always a strong function of the hydrogen concentration because the coke deposited over the Pt particles can be partially removed by reaction with hydrogen (9–11). Over a typical Pt-based dehydrogenation catalyst the rate of dehydrogenation has a negative half order with respect to hydrogen while the rate of deactivation is usually inversely proportional to the hydrogen concentration. Therefore, the performance ratio defined above would continuously increase as a function of the H_2/hydrocarbon ratio over a supported Pt catalyst. As discussed below, we ascribe these differences to the disparate nature of the coke deposits and their reactivity towards hydrogen over the two types of catalysts. That is, we propose that although over Pt catalysts the coke deposits are more easily removed by H_2, they result in greater deactivation than over sulfided nickel catalysts.

Effect of Preoxidation of the Catalysts before Sulfiding

We found that the reduction step prior to sulfidation was not necessary to obtain an active and selective catalyst. Actually, as shown in Table 3, a higher activity was observed when the catalyst had been oxidized before sulfidation. When we compared a catalyst prereduced in H_2 at 873 K for 1 hr and then sulfided with DMSO in H_2 (catalyst A) with the same material preoxidized in 4% O_2 in He at 623 K and then sulfided with DMSO in H_2 (catalyst F), we observed that the preoxidized catalyst was more active. We ascribe this activity enhancement to a better dispersion of the nickel sulfide resulting from the preoxidation treatment in comparison with the prere-

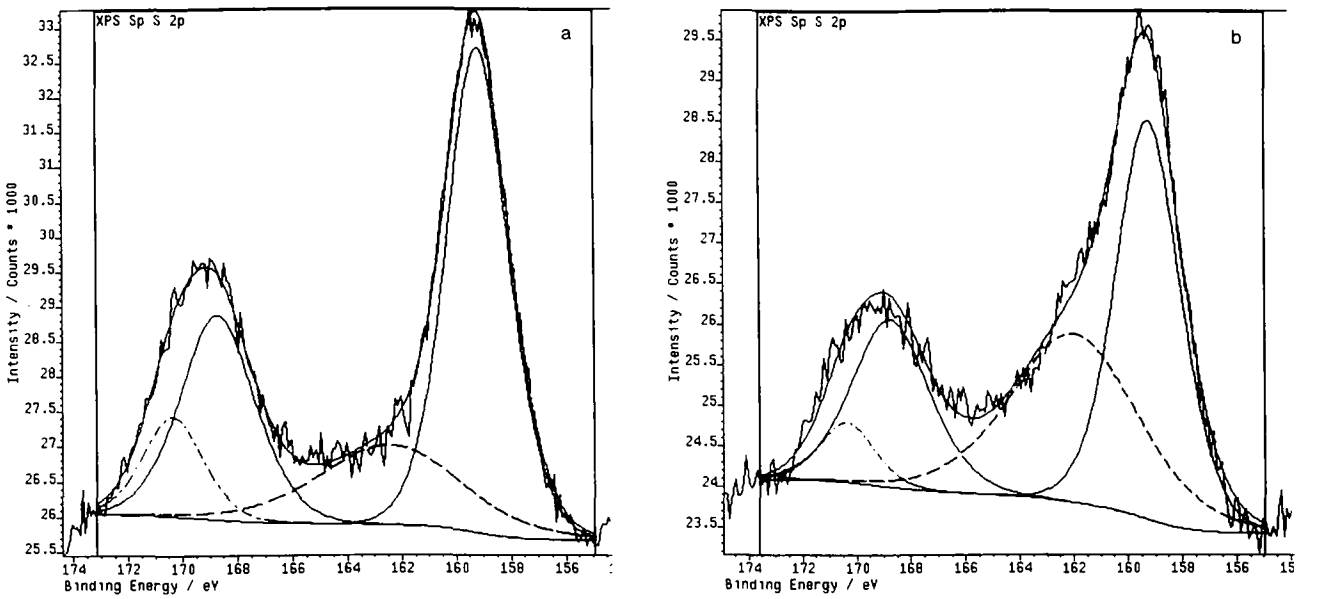

FIG. 4. XPS spectra in the binding energy range 155–174 eV. The observed peaks correspond to Cs (1*s*) and S (2*p*). The fitted curves correspond to Cs (—), S^{2-} (– –), and SO_4^{2-} (– · –). (a) Catalyst A (prereduced before sulfiding). (b) Catalyst F (pre-oxidized before sulfiding).

duction. Our hydrogen chemisorption measurements on nonsulfided samples showed that the dispersion of Ni on the Cs–alumina support rapidly decreased during the first minutes of reduction in hydrogen at 873 K. By contrast, when the reduction at 873K was eliminated, a significantly higher dispersion of the sulfided Ni was achieved.

Figure 4 shows the XPS spectra of the S(2*p*) region for catalyst A (Fig. 4a) and catalyst F (Fig. 4b). The pair of peaks at BE = 159.5 and 169.2 eV are attributed to Cs($4p_{3/2}$) and Cs($4p_{1/2}$), respectively, while the peaks at 170.5 and 162.3 eV are attributed to S(2*p*) of SO_4^{2-} and S^{2-} species, respectively. A more quantitative comparison appears in Table 3 which shows the XPS Ni($2p_{3/2}$)/Al(2*s*) and S^{2-}/Al(2*s*) ratios. These ratios indicate that the dispersion of Ni and S species is significantly higher on catalyst F, which exhibited the higher activity, than on catalyst A. The concentration of catalytically active species in catalyst F also may be greater than in catalyst A as indicated by the increase in the S^{2-}/Al(2*s*) ratio.

Rates of Carbon Formation

The rate of carbon deposition was measured in the Berty reactor on sulfided Ni catalysts under various conditions. Table 4 shows a comparison of the rates of carbon formation on sulfided Ni/Cs–alumina, catalyst E, at 873 K for H_2–isobutane and H_2–isobutylene gaseous mixtures. In agreement with the observed profiles in the flow reactor, the rate of carbon formation from isobutylene was much higher than that from isobutane. Under H_2–isobutane–isobutylene mixtures, the rate was roughly first order in the concentration of isobutylene. This dependence is shown in Fig. 5. These results suggest that the coke formation on these catalysts is mainly due to the dehydrogenation product, isobutylene, and does not strongly depend on the hydrogen concentration.

The observed coke profiles in the catalyst bed further support this conclusion. The concentration of deposited carbon on catalyst A at 873 K was measured at various positions in a fixed-bed flow reactor. The profile obtained after a reaction period of 10 h is depicted in Fig. 6 and shows that the deposition of coke increased with the distance from the inlet. This type of profile is typically observed in packed bed flow reactors when the coke precursor is the product.

The first order rate expression was used to compare the coking characteristics of the different catalysts investi-

TABLE 4

Comparison of Isobutane and Isobutylene as Coke Precursors

Gaseous mixture (molar ratio)	Time on stream (hr)	Carbon[a] (mg C/g cat)
isobutane/H_2 (1/1)	10	2.3
isobutylene/H_2 (1/1)	6	65.3

[a] Measured by the LECO method after contact with the gaseous mixture at 873 K in the Berty reactor.

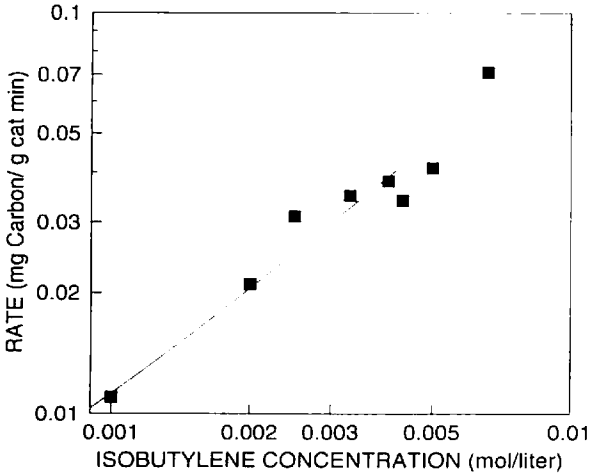

FIG. 5. Kinetics data obtained in the recirculating Berty reactor. Rate of coke formation as a function of isobutylene concentration in the feed.

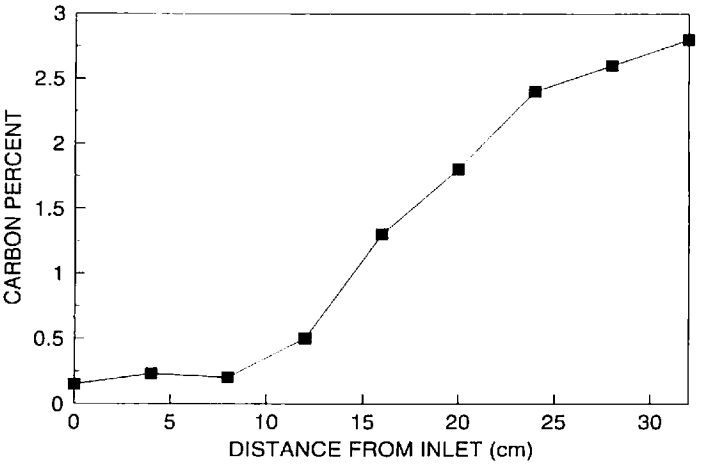

FIG. 6. Coke profile in a packed bed reactor. Carbon content (wt%) on the catalyst as a function of distance from the inlet after 10 hr under reaction conditions over catalyst A at 873 K and a H_2/isobutane molar feed ratio of 1/2.

gated. As illustrated in Table 5, the integrated values of the coking rate constants obtained during different runs on catalysts A and C are compared as a function of time on stream. Catalyst A, which was calcined and contained 5% Cs, exhibited a coking rate constant of about 10 (mg C/g cat. min)/(mol/l). This rate constant is *more than four orders of magnitude lower* than those obtained with unsulfided Ni catalysts.

Much smaller but still significant differences in the coking rates were obtained within the sulfided Ni series. For example, the coking rate constant on catalyst A was about one order of magnitude lower than on catalyst C, which only contained 3% Cs, and catalyst D, which was not precalcined. Furthermore, the coking rate constant for catalyst A did not vary as a function of time on stream while it rapidly decreased for catalysts C and D. We ascribe these differences to the acidity of the alumina support. Table 5 also shows the relative acidity as determined from TPD profiles of adsorbed pyridine for the three samples. It is clear that residual acidity on catalysts C and D was significantly higher than on catalyst A.

In addition to the differences in coking rates, this difference in residual acidity resulted in important differences in catalyst performance. The experiments reported in Table 5 demonstrated that catalyst A, for which the support acidity was minimal, exhibited high selectivy towards isobutylene. By contrast, catalysts C and D, on which we detected residual acidity, showed much lower selectivities due to contributions of cracking and isomerization products. At the same time, the residual acidity seemed to

TABLE 5

Effect of Residual Acidity of the Support on Product Distribution

Catalyst	Coking rate constant[a]	Relative acidity[b]	Product distribution (mol %)						
			C1	C2	C2 =	C3	C3 =	*n*C4	*i*C4 =
A	10[c]	1	5.2	0.4	0.2	1.8	3.3	0	89.1
	10.5[d]		5.8	0	0.2	1	3.2	0	89.8
C	210[c]	7	42.8	3.6	0.5	1.7	3	11.7	36.7
	56[d]		16.5	2.7	0.5	2.2	2.4	2.4	73.3
D	300[c]	9	36.5	4.3	1.4	4.1	3.3	12.2	38.2
	105[d]		17.3	3.6	1	2.7	3	10.2	62.2

[a] (mg carbon/g cat. min)/(mol *i*C4/liter).
[b] As measured by TPD of adsorbed pyridine.
[c] After 1 hr on stream.
[d] After 25 hr on stream.

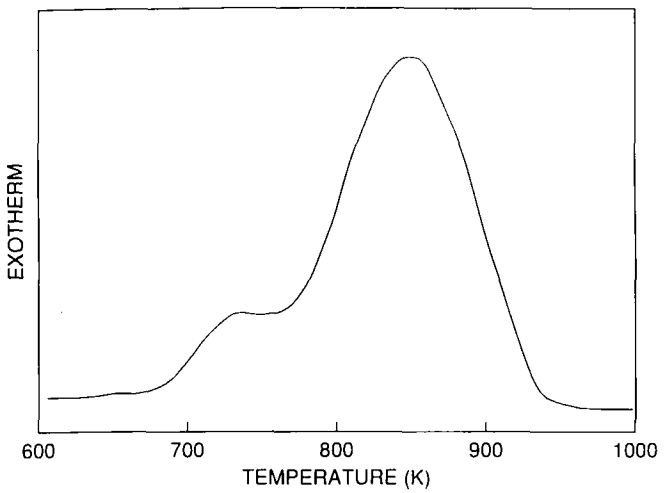

FIG. 7. Differential Scanning Calorimetry (DSC). Thermogram obtained during the oxidation of carbon deposits on catalyst A containing 6 wt% carbon. A prereduced and presulfided catalyst A sample without coke was used as a reference. Therefore, the observed exotherms are only due to the oxidation of coke.

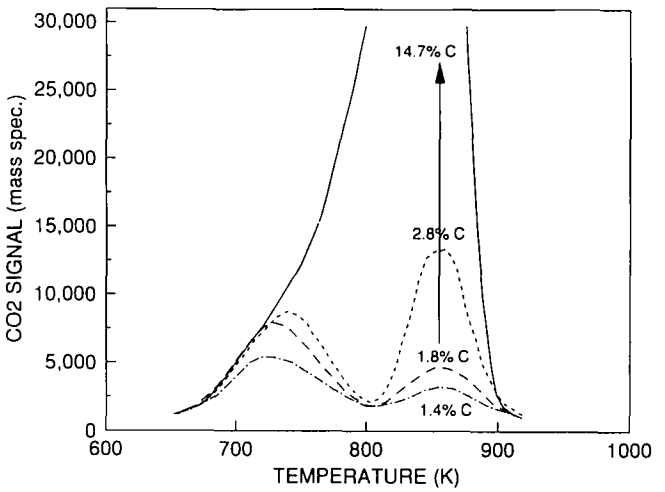

FIG. 8. Temperature Programmed Oxidation (TPO). Carbon dioxide profiles obtained on samples of catalyst A containing various amounts of carbon.

have had a detrimental effect on catalyst life. Due to the increased rate of coke formation, the catalysts registering acidity deactivated much more rapidly than those with no residual acidity. The observed rapid decline in the rate of carbon deposition in catalysts C and D as a function of time can also reasonably be ascribed to carbon blocking of the acid sites.

The particle size of the nickel species also had an effect on the rate of coke formation. As described above, the preoxidized and sulfided catalyst, F, displayed a much more highly dispersed nickel sulfide component than the prereduced and sulfided catalyst, A. Not only was catalyst F more active, as shown in Table 3, but it also formed coke at a lower rate than did catalyst A.

Characterization of the Coke Deposits

Differential scanning calorimetry was used to characterize the carbon deposits on a series of samples previously exposed to steady state reaction conditions for extended periods of time and which contained various amounts of carbon. The exotherms resulting from the combustion of coke in air were used to calculate the heat of combustion of the deposits. Figure 7 displays a typical DSC curve showing two exotherms at about 730 K and 860 K. The calculated heats of combustion resulting from the exotherms for several coked samples of catalyst A are summarized in Table 6. A clear trend is evident: the samples containing carbon deposits below 3–4 wt% had a heat of combustion higher than 110 kcal/mol of C, while

TABLE 6

Heat Evolved During Combustion of Coke Deposits as Determined by DSC

Amount of carbon (wt%)	Heat evolved (kcal/mol C)
1.8	120
2.3	115
6.1	85
14.7	90

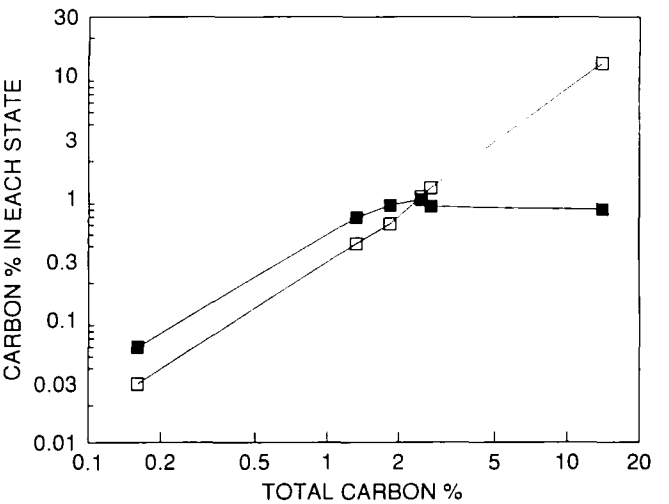

FIG. 9. Amount of carbon in each TPO state as a function of the total amount of coke. (■) Low temperature peak, activation energy = 45 kcal/mol (carbon I state). (□) High temperature peak, activation energy = 52 kcal/mol (carbon II state).

those containing relatively large amounts of carbon had a heat of combustion of about 90 kcal/mol of C. The latter value is equivalent to the heat of combustion of graphite, while the former may indicate that the coke contains some H associated with the carbon. In agreement with these results, the X-ray diffraction patterns of the samples containing carbon deposits in concentrations above 10 wt% indicated the presence of graphite.

To further characterize the nature of the carbon deposits, we used the method of temperature programmed reaction (with oxygen, TPO, and with hydrogen, TPR) on several coked samples. The TPO profiles of this series, measured by monitoring the quadrupole mass selective detector signal corresponding to carbon dioxide as a function of temperature, are shown in Fig. 8. Two distinct CO_2 peaks resulting from the combustion of the carbon deposits were observed at 730–750 K and 860 K, in close correlation with the DSC data. We believe that they correspond to different states of carbon on the catalyst (carbon I and carbon II, respectively).

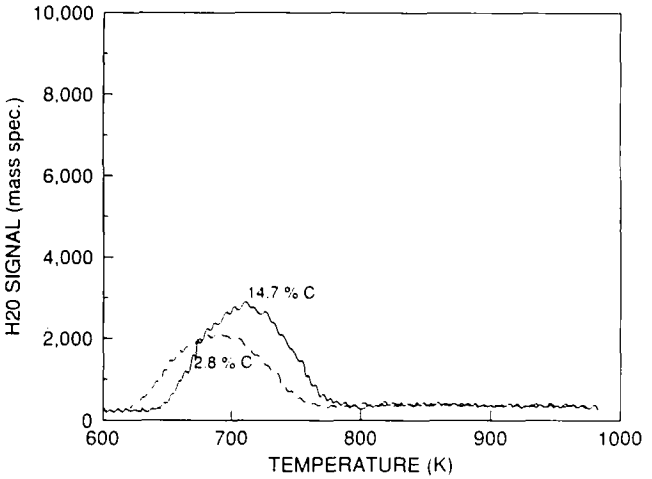

FIG. 10. Temperature Programmed Oxidation (TPO). Water profiles obtained on samples of catalyst A containing different amounts of coke.

To quantify the amount of carbon in each state, we fitted the experimental data with a rate expression which is first order in the amount of unburned carbon and used the activation energy and the relative carbon density in each state as adjustable parameters. The oxygen consumption was small in comparison to the oxygen concentration, which was assumed to be constant throughout the experiment. The best fit resulted for activation energies values of 45 and 52 kcal/mol for the carbon I and carbon II states, respectively. The distribution of carbon between each state calculated from the kinetics model is plotted in Fig. 9 as a function of the total amount of coke. At

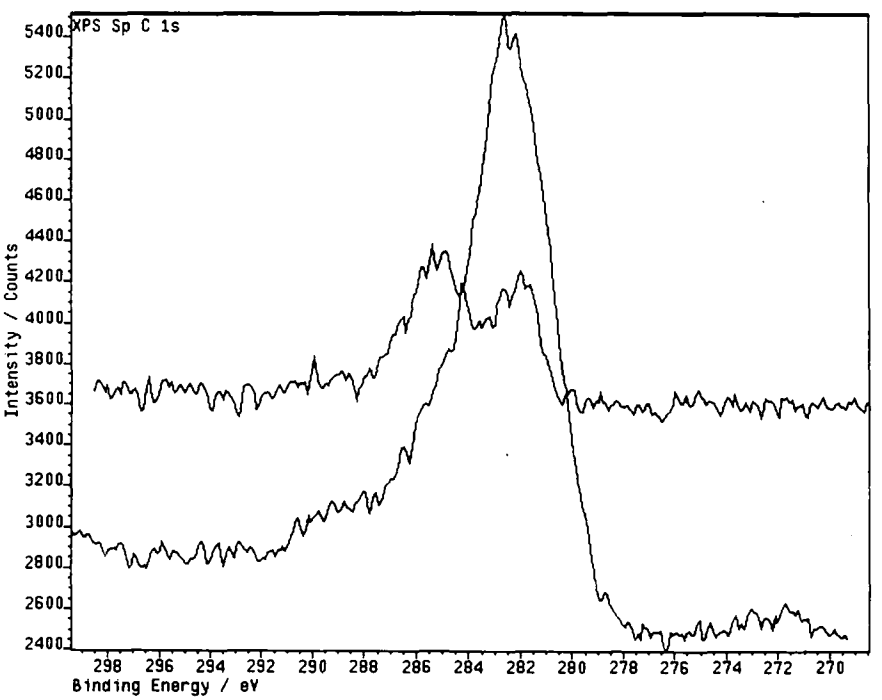

FIG. 11. XPS spectra in the binding energy range 270–298 eV. The observed peaks correspond to different states of C (1*s*). Upper spectrum: catalyst containing 1.5 wt% carbon. Lower spectrum: catalyst contining 13.8 wt%.

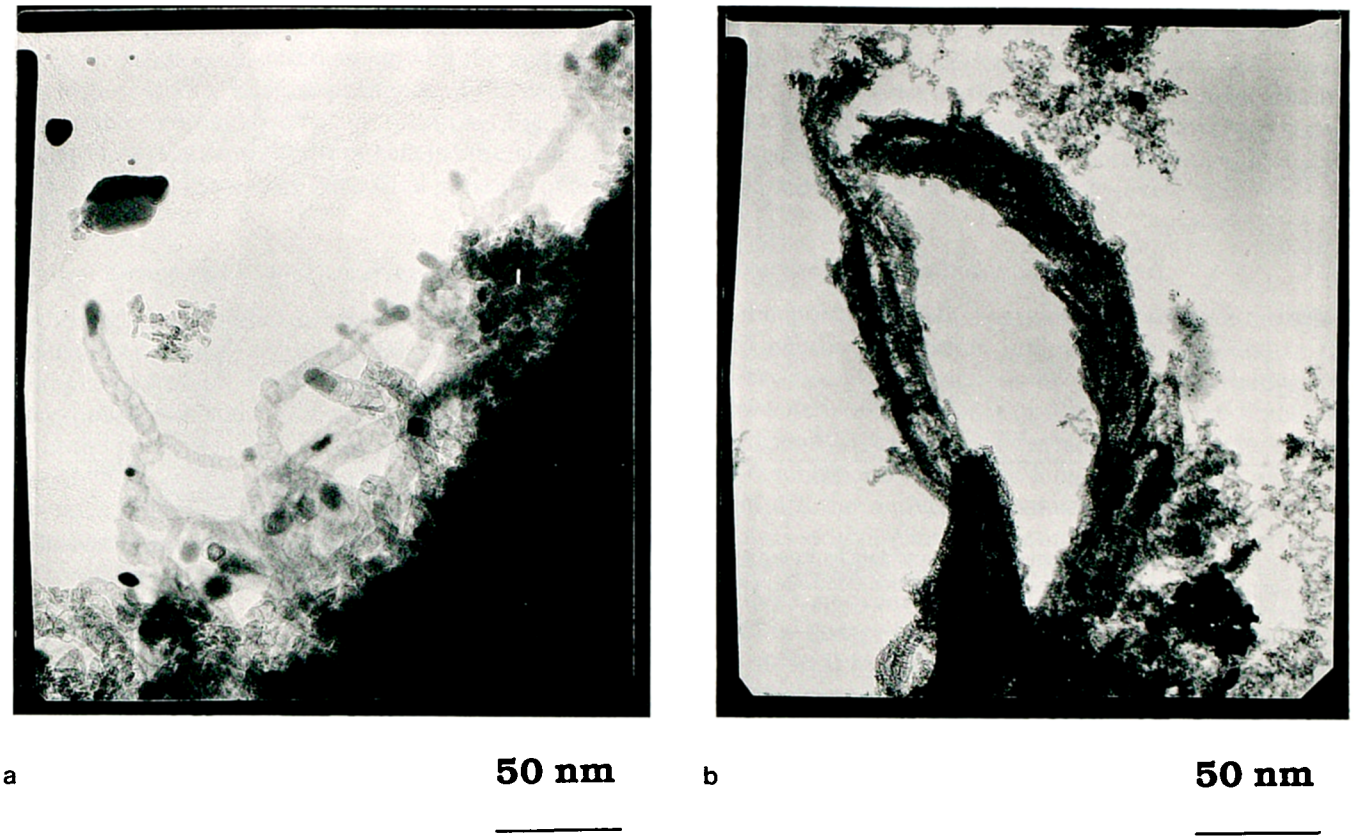

FIG. 12. TEM micrographs of heavily coked samples. Catalyst A containing 29 wt% carbon. (a) Carbon filaments containing a nickel particle at the end. (b) Branched carbon filaments.

low carbon contents, both states increased simultaneously, but when the total amount of carbon reached about 2–3 wt%, the carbon I state seemed to saturate while the carbon II state continued to increase. The saturation value of the carbon I (about 1 wt%) corresponds to a C/Ni molar ratio near unity. It is noteworthy that when this saturation value was reached, the catalyst exhibited its maximum dehydrogenation activity. As shown in Fig. 2, the maximum activity of catalyst A in the flow reactor occurred at about 9 hr on stream. From the kinetics data of coke formation, the amount of carbon deposited on that catalyst at any time can be readily calculated. In this case, we used a reaction constant of 10 (mg C) (g cat min)$^{-1}$ (mol/l)$^{-1}$ and assumed a linear increase in the isobutylene concentration with time during the activation period. Under these conditions the estimated total amount of carbon on the catalyst after 9 hr on stream would be 2.7 wt%, nearly the same amount of total carbon at which the saturation of the carbon I was reached. This correspondence suggests that the catalytic induction may be related to the formation of the carbon I state.

To determine the amount of hydrogen associated with the C in the coke, we measured the H_2O evolved during the combustion of the carbonaceous deposits. The evolution of H_2O as a function of temperature is depicted in Fig. 10. The amount of H_2O evolved was very small in comparison to the amount of CO_2; it appeared at relatively low temperatures; and it did not increase with an increase in the content of carbon. As a consequence, the H/C ratio in the carbonaceous deposits of the catalyst containing 2.8 wt% C was about 0.2, while it only was 0.04 in the case of the catalyst containing 14.7 wt% C.

X-Ray Photoelectron Spectroscopy (XPS) was used to identify the different carbonaceous species present in the coke. As shown in Fig. 11 the XPS spectra show two different carbon states on the catalysts with low amounts of coke but essentially one dominant feature when the amount of carbon deposited becomes large. In the first case, the two carbon states can be ascribed to carbidic carbon (282 eV) and partially hydrogenated carbon species, CH_x (285 eV). The dominant feature at high carbon contents can be described as graphitic carbon (283 eV). These results are in agreement with the XRD, TPO, and DSC data that show that on the lightly coked catalyst the

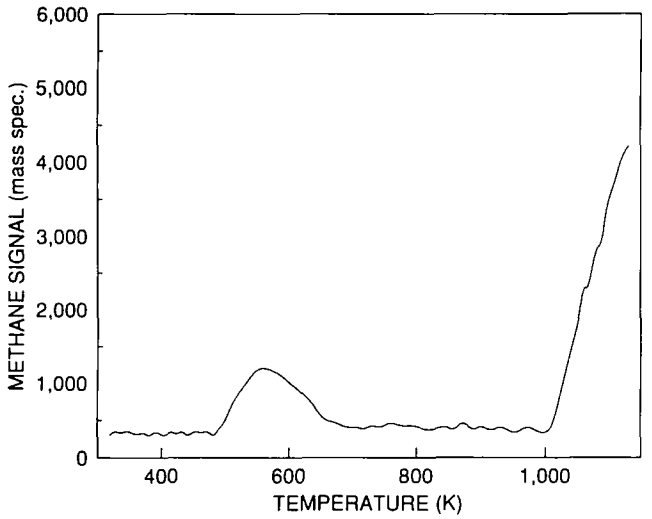

FIG. 13. Temperature Programmed Reaction of pure hydrogen with a coked sample of catalyst A containing 29 wt% carbon. Methane profile as a function of temperature.

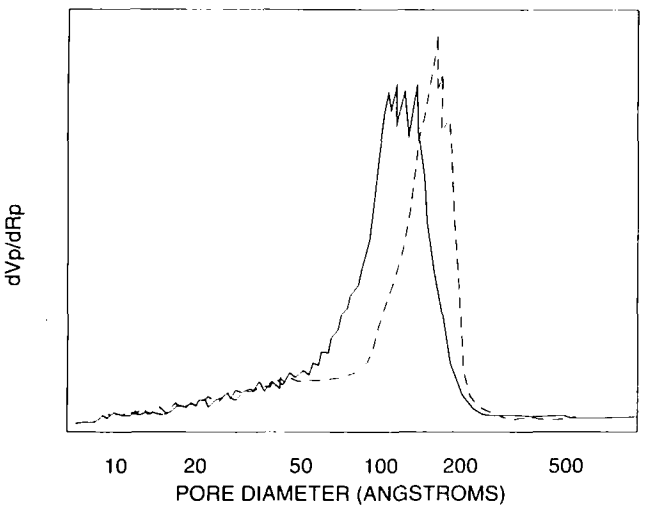

FIG. 15. Pore size distribution as measured by nitrogen desorption porosimetry. (—) Catalyst A. (– –) Catalyst B.

carbon contains some hydrogen and is more reactive, while on the more heavily coked samples the carbon contains almost no hydrogen and is refractory and graphitic in nature.

Filamentous carbon deposits were observed by TEM on coked catalysts containing more than 20 wt% C. As previously observed by other authors (12), some of the filaments had a rather uniform shape and contained a high contrast particle at their end. The second type of filament observed was less uniform and seemed to grow in branches from an initially common filament. These types of filaments have been typically observed on heavily sulfided catalysts (13–15). Figure 12 illustrates the two different types of filaments.

The TPR profile obtained on a heavily coked catalyst (29 wt% C) is shown in Fig. 13. Two main peaks were observed: a small peak at 540 K and a larger one at about 1090 K. It is interesting to note that the amount of carbon that may be removed from the catalyst with hydrogen is small; the LECO measurements indicated that the carbon left on the catalyst after the TPR experiment was 90% of the initial amount. This result demonstrates the refractory nature of the carbon deposits toward hydrogen, which contrasts with a much higher reactivity observed on unsulfided Ni catalysts. For example, McCarty *et al.* (16) have found that filamentous carbon deposited on unsulfided Ni/Al_2O_3 catalysts readily reacts with pure H_2 in the tem-

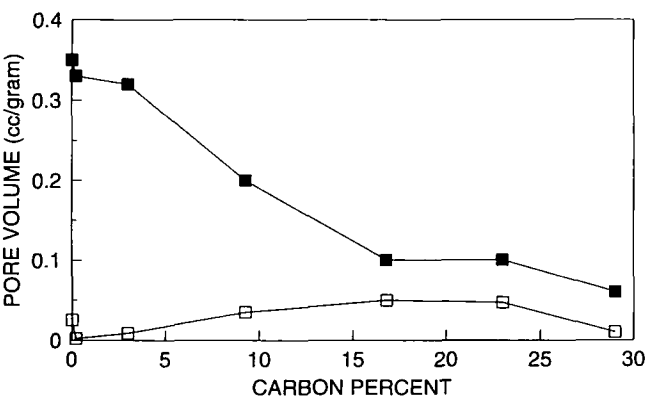

FIG. 14. Variation of the pore volume available to the gas phase as a function of the amount of carbon deposited on a sample of catalyst A. (■) Pore size range = 10–20 nm. (□) Pore size range < 6 nm.

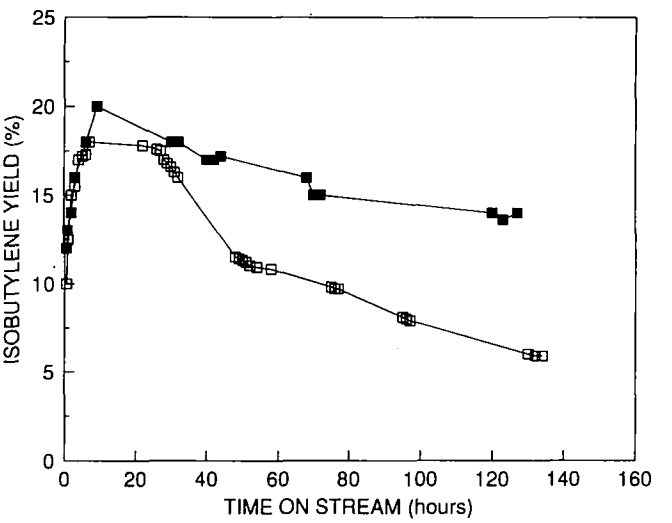

FIG. 16. Evolution of activity as a function of time on stream. H_2-isobutane reaction (molar ratio 1/2) at 873K in the flow reactor. (■) Catalyst B. (□) Catalyst A.

perature range 700–1000 K, with a maximum reaction rate at 875 K. When considered along with the activity data, which show only a weak dependence of the deactivation rate on the hydrogen/isobutane ratio (see Fig. 3), these results show that there is little benefit in life characteristics to be gained by increasing the partial pressure of feed hydrogen.

Catalyst Deactivation by Pore Plugging

Although the buildup of carbon deposits is slow on sulfided nickel catalysts, when the amount of carbon becomes large we have observed evidence for pore plugging corresponding to catalyst deactivation. As shown in Fig. 14, in the particular case of the catalyst A, that situation started when the amount of carbon reached 5 wt% C. At that point, the pore volume in the size range 10–20 nm started to decrease while that in the small pore range increased due to the development of porosity of the carbon deposits.

The effect of pore structure of the support on catalyst life can be observed by comparing the deactivation patterns of catalysts A and B. The pore size distributions of the two samples are compared in Fig. 15. Catalyst B, prepared using a support which had been subjected to a leaching treatment with a solution of oxalic acid, exhibited a much larger median pore diameter than the standard catalyst A. This difference in pore structure resulted in an important improvement in catalyst life. As shown in Fig. 16, catalyst B presented a much lower rate of deactivation than catalyst A when compared at the same initial conversions. It must be noted that on catalyst B the decrease in pore volume in the 10–20 nm range only started when the amount of carbon reached about 10 wt%. Both samples exhibited about the same metal dispersion (H/Ni = 0.35) after reduction at 873 K and prior to sulfidation. Therefore, the difference in deactivation rate was not related to a different particle size of the sulfided Ni species that would result in a different rate of carbon formation but rather to an increase in the coke tolerance of catalyst B.

IV. DISCUSSION

We have demonstrated that sulfided Ni catalysts can be very selective and stable for the dehydrogenation of isobutane. These catalysts exhibit some unique characteristics which influence both the course of the dehydrogenation reaction and the mechanism of their deactivation. It is interesting to note that under the same reaction conditions, but without sulfiding, the supported Ni catalysts described here only produce methane due to the high activity of Ni for hydrogenolysis. In addition to its effect on hydrogenolysis, sulfur has a twofold effect with regard to coke formation. On the one hand, as shown in Fig. 1, it drastically reduces the rate of carbon deposition. But, on the other hand, as demonstrated in the TPR experiments, it also reduces the rate of carbon gasification by hydrogen. Therefore, on sulfided nickel catalysts there is no advantage to increasing the concentration of hydrogen in the feed beyond a relatively low level.

Dehydrogenation Reaction Mechanisms

An important question to address is whether the selectivity improvement after sulfiding is simply due to the supression of side reactions or rather to the generation of new dehydrogenation sites. We recall the tenet that hydrogenolysis of alkanes over metals is a structure sensitive reaction and requires a large ensemble of atoms to constitute the active site, while dehydrogenation over metals is structure insensitive and does not require a large ensemble. Some authors have even proposed that this reaction can occur on a single metal atom site [17].

At low dosage levels, S binds very strongly to the surface of Ni. It has been shown (18) that the heat of formation of chemisorbed S on Ni is more negative than the heat of formation of the most stable bulk sulfide Ni_3S_2. This energy difference generates a driving force for the segregation of sulfur to the surface and, consequently, for the stabilization of sulfided nickel surfaces. Surface science studies (19) on well characterized single crystals have identified distinct S/Ni patterns in which the chemisorbed S occupies fourfold hollow sites.

Several authors have reported the effect of S on the catalytic and chemisorptive properties of Ni single crystals. The presence of S greatly reduces the saturation coverage of hydrogen on Ni surfaces (20). This change has been ascribed to a steric hindrance to hydrogen recombination rather than to a modification of the electronic structure induced by the adsorbate. In like manner, it has been proposed that the main effect of S on the adsorption of CO (23) or of methane (24) is caused by simple site blocking. Similar decreases in saturation coverage and desorption kinetics parameters have been observed for other foreign species on the surface such as carbon (21, 22).

Based on this premise alone it would be reasonable to expect that partial blocking of the surface should significantly improve the selectivity towards dehydrogenation at the expense of hydrogenolysis. However, in the studies cited above, the S/Ni system could be described as a metal surface partially poisoned by the presence of adsorbed S. In the catalysts of the type described herein the sulfidation depth is much greater and most of the Ni is in the +2 oxidation state. The behavior of the highly sulfided nickel catalysts of this study is best explained by regarding the surface which is catalytically active and selective towards dehydrogenation of alkanes *not simply as a modified zero-*

valent metal but as a discrete stoichiometric compound with quite different catalytic properties from those of dispersed metallic nickel. In fact, we have demonstrated that the reduction of Ni is not a prerequisite for obtaining active and selective catalysts. Therefore, we propose that differences among various catalyst preparations in our study are largely related to the degree of formation and surface exposure of this compound and that the catalytic cycle may require the intimate participation of ligands on nickel atoms as hydrogen transfer sites.

The analysis of the activation periods observed on the sulfided Ni/Cs–Al_2O_3 catalysts suggests that a mode of action other than that observed over clean metallic surfaces is favored and may shed light into the nature of the active phase. The activity increase in the inchoative stages of the reaction only is observed when the initial level of conversion is high. This may suggest that the activation period is caused by the interaction of the product, isobutylene, with the sulfided surface. The saturation behavior observed in the TPO experiments further suggests that the maximum of activity is achieved when the concentration of the more reactive carbon I state reaches its maximum. This behavior contrasts sharply to that of unsulfided Pt catalysts (see Fig. 2), implying a difference in mechanism over these different surfaces.

Activation periods such as those reported in this study are common in heterogeneous catalysis (25). Some possible causes of activation proposed in the literature are the formation of active carbon species (26–30), the increase in active surface area (31), and the creation of surface defects (32). One or more of these might contribute to the activation behavior exhibited by the sulfided Ni catalysts.

Consider first that an active carbon species, such as the carbidic carbon produced by the decomposition of isobutylene during the activation period, might participate in the catalytic reaction cycle. Fujimoto and co-workers (28–30), studying the dehydrogenation of cyclohexane and isopentane on carbon-supported metal catalysts, have proposed that carbon may play a direct role in the dehydrogenation reaction. They suggest that the alkane activation takes place on the carbon itself and the role of the metal is to act as a port for releasing the hydrogen produced. Thomson and Webb (33) also have proposed a mechanism in which carbonaceous species on the surface participate in the active site as hydrogen transfer agents.

One elaboration of these ideas would be that the alkane be activated on a Ni atom site while a bound carbon ligand (carbidic C) may act as an acceptor of hydrogen released during the dissociative adsorption. The formation of the nickel–carbidic C species may occur during the activation period and the maximum activity then would be reached when the nickel–carbon species approached its maximum concentration. The saturation value of such a moiety, as observed in our TPO experiments (identified as the carbon

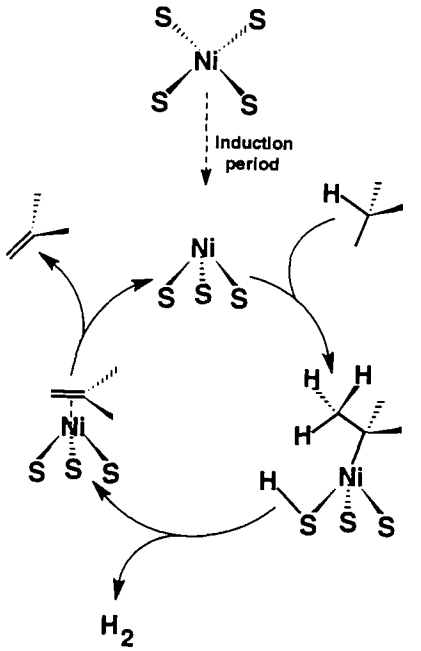

SCHEME I

I state), would correspond to a C/Ni molar ratio of about unity in the catalysts of interest here.

However attractive the evocation of such an organometallic species may be as an explanation of the nature of the catalytic cycle, it does not account for the role of sulfur in the system. An alternative mechanism that would explain both the observed activation period and also the role of sulfur may be represented as follows. Initial sulfiding probably results in the formation of a nickel sulfide

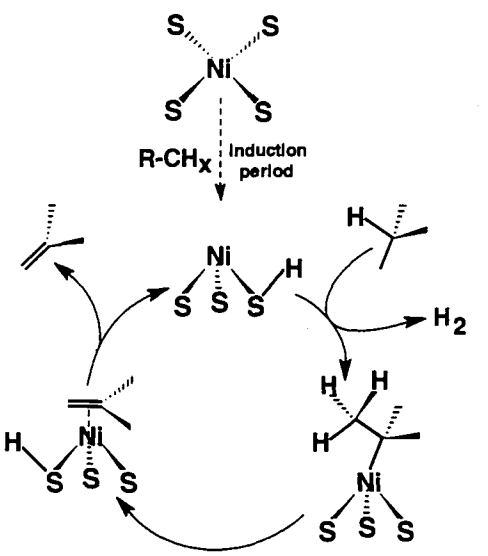

SCHEME II

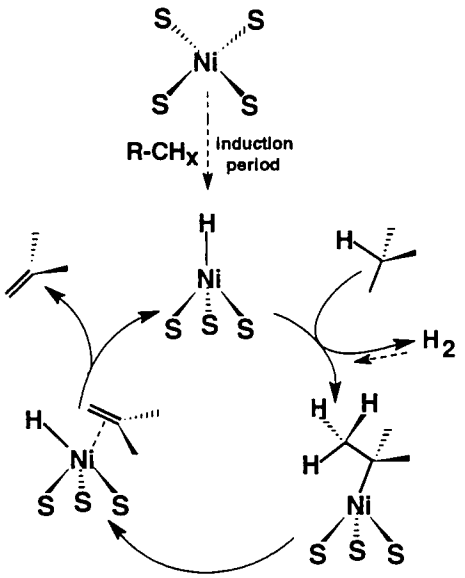

SCHEME III

surface compound. A modification of the sulfided nickel surface by interaction with isobutylene could result in the creation of sulfur vacancies on the surface thereby increasing the coordinative unsaturation of S-ligated Ni during the activation period. A similar sequence has been suggested by Takeuchi *et al.* (34, 35), who have observed that sulfided Ni is initially inactive for olefin hydrogenation and H_2–D_2 exchange but becomes active after being in contact with acetylene.

Based on this idea, we propose a catalytic cycle as depicted in Scheme I. The active species containing coordinatively unsaturated Ni–S sites would be formed by interaction with the reaction mixture, perhaps through the intermediacy of a labile nickel–carbidic species. Once formed, the three-coordinate Ni–S entity would be able to dissociatively adsorb isobutane, leaving the H bonded to a sulfur atom. By β-hydrogen radical transfer, a second H could combine with the one at the bound sulfur site, leading to the evolution of molecular hydrogen into the gas phase and the generation of a π-bonded alkene intermediate. In the final step, the olefin would desorb, regenerating the active site. This scheme would account for the observed activation period, the first order dependence on isobutane, and the zero order dependence on hydrogen concentration observed for dehydrogenation.

Alternatively, the dominant site of the resting state could be pictured as already containing a S-bound H atom, Scheme II. The persistence of this surface entity might be further bolstered by an agostic interaction of the S-bound hydrogen with the nickel atom (36, 37). This resting state species would favor a concerted release of H_2 and σ-bonding of the alkane followed by formation of a π-bonded alkene.

It is less likely that the catalytic cycle directly involves a nickel hydride species (Scheme III) since dehydrogenation mechanisms based on such hydrides would be expected to display a negative reaction order with respect to the hydrogen partial pressure, which was not observed here.

Catalyst Deactivation

The stability of these catalysts is related to the nature of the interaction of the sulfided nickel with coke precursors. Our results are consistent with the hypothesis that the global mechanism of coke formation on the sulfided nickel catalysts is similar to that on unsulfided nickel, but at a much lower rate. It must be noted that in this case the level of sulfur present on the catalyst is significantly higher than in many other studies in which the system was considered as a zero-valent metal partially covered by sulfur. In those cases the rate of coke formation is not so greatly reduced and in some cases it may even increase (13).

Although several types of coke can be differentiated by their location, their physical form, and their hydrogen contents, all cokes seem to have a common precursor: the process of carbon deposition is initiated largely by the decomposition of isobutylene, which is the main source of coke, as demonstrated by the experiments described above. During the initial stages of carbon deposition, carbidic and partially hydrogenated carbon species could form on the sulfided nickel particles. A surprising characteristic of these catalysts is that the process of deposition of the initially formed carbonaceous species does not result in any decrease in the dehydrogenation activity but rather in an increase as described above.

When carbon content reaches high levels, formation of filamentous carbon is observed. The most widely accepted physical mechanism for the formation of carbon filaments on metallic Ni catalysts involves the decomposition of the hydrocarbon on the surface followed by bulk diffusion of carbon through the metallic crystallite and precipitation at the rear end, possibly at a crystal dislocation, leaving the active surface exposed but connected to a long filament (12, 38). Unless a graphitic sheath completely encapsulates the particle, the catalytic surface remains active during the entire cycle of carbon formation.

Although perhaps differing in the detail of how chemical intermediates leading to highly dehydrogenated coke are formed, we propose that a similar gross physical mechanism is active on sulfided nickel for carbon filament formation as proposed for metallic nickel (14, 15). This characteristic may account, in part, for the relatively high stability of these catalysts under severely deactivating conditions. However, the formation of carbon filaments would eventually result in deactivation by plugging of the porous support. To overcome this problem we have

modified the pore structure in a way that improved catalyst life by reducing the tendency toward pore plugging (see Fig. 16).

The mechanism of coke formation is an important difference exhibited by sulfided nickel catalysts in comparison with unsulfided Pt catalysts. On Pt catalysts, it is necessary to operate at relatively high H_2/hydrocarbon ratios in order to keep the metal surface clean of carbon deposits. It has been shown that small amounts of coke may cover a large fraction of the metal surface making it unavailable to reactants. For example, on a 0.1 wt% Pt/Al_2O_3 catalyst, a C/Pt molar ratio of 1.0 is enough to render half of the total metallic surface area unaccesible (39). By contrast, on the sulfided nickel catalysts described here, the maximum activity is reached when the C/Ni molar ratio is about 1.0.

Some of the commercially utilized isobutane dehydrogenation catalysts (40–42) are based on Pt and their rate of coke formation is strongly affected by the H_2/hydrocarbon ratio. The addition of metal promoters such as Sn to the Pt catalysts significantly improves the tolerance to coke. As shown by Lin *et al.* (43), the same level of carbon deposition that causes a deactivation of 90% of the metal surface in an unpromoted Pt catalyst only causes a 70% deactivation in a Sn-promoted one. On a Pt–Sn catalyst the migration of the carbon deposits from the metal to the support would be easier than on an unpromoted Pt catalyst, which would help to reduce the amount of carbon left on the metal. However, as described by Loc *et al.* (9), the process of clearing the metal particles requires the use of hydrogen. As a consequence, even the promoted Pt catalysts (40–42) require higher dilution ratios than the ones at which the sulfided nickel catalysts operate best.

CONCLUSIONS

We have studied the dehydrogenation of isobutane to isobutylene over sulfided Ni catalysts. Treatment of nickel catalysts with sulfur-containing reagents resulted in dramatically improved selectivity and decreased rates of coke formation. By proper sulfiding, adjusting the pore structure, and reducing the acidity of the support, very active, selective, and stable catalysts were obtained. These catalysts were able to operate for relatively long reaction periods without regeneration under very low hydrogen/hydrocarbon ratios. The use of the sulfided Ni catalysts at low hydrogen feed content in commercial dehydrogenation processes might result in a new technological alternative which could effect improved economics based on reduction of compression requirements and higher equilibrium conversions.

The catalysts exhibited induction periods in activity of several hours until a maximum was reached. Two alternative explanations for the activation process were discussed. The first one considers the participation of a nickel–carbidic C complex in the reaction scheme. The second one considers the creation of sulfur vacancies during the initial coke deposition period which would increase the exposure of a catalytically active Ni–S moiety.

From the point of view of practical applications it is worth noting that particular preparations of sulfided nickel catalysts can remain on stream for several days under severely deactivating conditions of low H_2/hydrocarbon ratios and high temperatures, yet still be highly active for dehydrogenation.

ACKNOWLEDGMENTS

We thank Eugene Coggins and John Mumford for conducting reactor studies and Sun Company, Inc., for permission to publish this work.

REFERENCES

1. Chang, E. *in* "Alkane Dehydrogenation and Aromatization," Report No. 203. SRI International, CA, Menlo Park, 1992.
2. Horsley, J. A., *in* "Catalytic Dehydrogenation and Oxidative Dehydrogenation," Catalytica Study No. 4190 DH. Catalytica, CA, Mountain View, 1991.
3. Rennard, R. J., and Freel, J., *J. Catal.* **98,** 235 (1986).
4. Kim, C., and Somorjai, G. A., *J. Catal.* **134,** 179 (1992).
5. Rostrup-Nielsen, J. R., and Alstrup, I., *in* "Catalysis 1987" (J. W. Ward, Ed.) p. 725. Elsevier, Amsterdam, 1988.
6. Rostrup-Nielsen, J. R., *J. Catal.* **85,** 31 (1984).
7. Alstrup, I., Rostrup-Nielsen, J. R., and Roen, S., *Appl. Catal.* **1,** 303 (1981).
8. Zwahlen, A. G., and Agnew, J. B., *Ind. Eng. Chem. Res.* **31,** 2088 (1992).
9. Loc, L. K., Gaidai, N. A., Gudkov, B. S., Kiperman, S. L., and Kogan, S. B., *Kinet. Katal.* **27,** 1365 (1986).
10. Loc, L. K., Gaidai, N. A., Gudkov, B. S., Kostyukovskii, M. M., Kiperman, S. L., Podkletnova, N. M. Kogan, S. B. and Bursian, N. R. *Kinet. Katal.* **27,** 1371 (1986).
11. Loc, L. K., Gaidai, N. A., and Kiperman, S. L., *in* "Proceedings, 9th International Congress on Catalysis, Calgary, 1988" (M. J. Phillips and M. Ternan, Eds.), Vol. 3, p. 1261. Chem. Institute of Canada, Ottawa, 1988.
12. Baker, R. T. K., and Harris, P. S., *in* "Chemistry and Physics of Carbon" (P. L. Walker, Jr., and P. A. Thrower, Eds.), Vol. 14, p. 83. Dekker, New York, 1978.
13. Baker, R. T. K., paper presented at the 13th North American Meeting of the Catalysis Society, Pittsburgh, May, 1993.
14. Rostrup-Nielsen, J. R., and Pedersen, K., *J. Catal.* **59,** 395 (1979).
15. Rostrup-Nielsen, J. R., *J. Catal.* **27,** 343 (1972).
16. McCarty, J. G., Hou, P. Y., Sheridan, D., and Wise, H., *in* "Coke Formation on Metal Surfaces" (L. F. Albright and R. T. K. Baker, Eds.), ACS Symposium Series, No. 202, p. 253. Amer. Chem. Soc. Washington, 1982.
17. Biloen, P., Dautzenberg, F. M., and Sachtler, W. M. H., *J. Catal.* **50,** 77 (1977).
18. McCarty, J. G., and Wise, H., *J. Chem. Phys.* **72,** 6332 (1980).
19. Perderau, M., and Oudar, J., *Surf. Sci.* **20,** 80 (1970).
20. Johnson, S., and Madix, R. J., *Surf. Sci.* **108,** 77 (1981).
21. Madix, R. J., *Catal. Rev. Sci. Eng.* **15,** 293 (1977).

22. Ko, E. I., and Madix, R. J., *Appl. Surf. Sci.* **3,** 236 (1979).
23. Benziger, J., and Madix, R. J., *Surf. Sci.* **94,** 119 (1980).
24. Goodman, D. W., *J. Vac. Sci. Technol. A* **2,** 873 (1984).
25. McAllister, P., and Wolf, E. E., *J. Catal.* **138,** 129 (1992).
26. Bukur, D. B., Mukesh, D., and Patel, S. A. *Ind. Eng. Chem. Res.* **29,** 194 (1990).
27. Kivila, C. S., Stair, P. C., and Butt, J. B., *J. Catal.* **118,** 299 (1989).
28. Fujimoto, K. and Toyoshi, S., *in* "New Horizons in Catalysis" (T. Seiyama and K. Tanabe, Eds.), Vol. 7A, p. 235. Elsevier, Amsterdam, 1981.
29. Asaoka, S., Masamizu, K., Fujimoto, K., and Kunugi, T., *J. Chem. Soc. Jpn.*, 1293 (1975).
30. Fujimoto, K., Masamizu, K., Asaoka, S., and Kunugi, T., *J. Chem. Soc. Jpn.*, 1062 (1976).
31. McAllister, P., and Wolf, E. E., *Carbon* **30,** 189 (1992).
32. Jnioui, A., Eddouasse, M., Amariglio, A., Ehrhardt, J. J., Alnot, M., Lambert, J., and Amariglio, H., *J. Catal.* **106,** 144 (1987).
33. Thomson, S. J., and Webb, G., *J. Chem. Soc. Chem. Commun.*, 526 (1976).
34. Takeuchi, A., Tanaka, K. I., Toyosima, I., and Miyahara, K., *J. Catal.* **40,** 94 (1975).
35. Takeuchi, A., Tanaka, K. I., and Miyahara, K., *J. Catal.* **40,** 101 (1975).
36. Garin, F., and Maire, G., *Acc. Chem. Res.* **22,** 100 (1989).
37. Brookhart, M. and Green, M. L. H., *J. Organomet. Chem.* **250,** 395 (1983).
38. Rostrup-Nielsen, J. R., and Trimm, D. L., *J. Catal.* **48,** 155 (1977).
39. Barbier, J., Marecot, P., Martin, N., Elassal, L., and Maurel, R., *in* "Catalyst Deactivation" (B. Delmon and G. F. Froment, Eds.), p. 53. Elsevier, Amsterdam, 1980.
40. Antos, G. J., U.S. Patent 4,216,346 (1980).
41. Wilhelm, F. C., U.S. Patent 3,998,900 (1976).
42. Miller, S. J., U.S. Patent 4,727,216 (1988).
43. Lin, L., Zhang, T., Zang, J., and Xu, Z., *Appl. Catal.* **11,** 647 (1990).